

Corrosion resistance of anodised single-phase Mg alloys

Zhiming Shi, Guangling Song^{*}, Andrej Atrens

CRC for Cast Metals Manufacturing (CAST), Division of Materials, School of Engineering, The University of Queensland, Qld 4072, Australia

Received 4 February 2005; accepted in revised form 10 November 2005

Available online 3 January 2006

Abstract

This work studied the effect of the impurity iron and the alloying elements aluminium and zinc in single-phase substrate magnesium alloys on the corrosion resistance of the alloys after anodisation. It was found that increasing zinc content (0–2%) led to increased corrosion resistance of an anodised single-phase Mg–Zn alloy. The addition of Al lowered the corrosion resistance of an anodised commercial purity Mg–Al single-phase alloy, whereas the same addition was found to be beneficial to the corrosion resistance of an anodised high purity Mg–Al single-phase alloy. Heat-treatment made the substrate Mg–Al and Mg–Zn alloys more uniform and hence improved the corrosion resistance of the alloys after anodisation. The detrimental effect of iron impurity on corrosion performance of the unanodised substrate single-phase magnesium alloys was inherited by the anodised alloys. The corrosion resistance of the anodised Mg alloys was found to be closely correlated with the corrosion performance of the unanodised as-cast Mg alloys.

© 2005 Elsevier B.V. All rights reserved.

Keywords: Magnesium alloy; Corrosion; Anodisation; Coating

1. Introduction

Anodisation treatments are used to improve the corrosion and wear resistance of magnesium alloys [1–12]. Most prior studies on anodisation of magnesium alloys have been focused on the effect of the anodisation process on the performance of the anodised alloys [8,13–17]. It has been found that the corrosion resistance of an anodic coating can be different on different magnesium alloys [18,19]. For example, an anodised Mg–Al alloy containing β phase had lower corrosion resistance than an anodised Mg containing no β phase [20] even though they were anodised under the same conditions. This finding indicates that the phase constituents can affect the corrosion resistance of an anodised magnesium alloy. This paper aims to understand the influence of the α matrix on the corrosion resistance of anodised magnesium alloys containing impurity element iron and alloying elements zinc and aluminium.

2. Experimental

2.1. Alloys

Commercial purity magnesium (CP-Mg) and high purity magnesium (HP-Mg) were used for comparison purposes and also as raw materials for producing Mg–Al and Mg–Zn alloys in this study. HP-Mg or CP-Mg ingots were melted in a ceramic crucible at 710 °C under protection of a cover gas, then pre-heated pure aluminium or zinc ingots were added to the molten Mg. After the alloying elements Al or Zn had been melted completely and mixed fully by stirring, the molten Mg alloy was cast into a coated iron mould. The chemical compositions of the produced alloys were analysed by Atomic Emission Spectroscopy (AES) and are listed in Table 1. Due to the different purities of the magnesium ingots used in production, the alloys had two different purities (denoted as commercial purity <CP> and high purity <HP>). CP-Mg, CP-Mg1Al, HP-Mg and HP-Mg1Al are specifically designated to identify their purity levels in this paper. The Mg–Zn alloys contained 0.5% Zn (Mg0.5Zn), 1% Zn (Mg1Zn) and 2% Zn (Mg2Zn) and the Mg–Al alloys contained 1% Al (Mg1Al), 5% Al (Mg5Al) and Mg10Al (10% Al). A group of the Mg–Al and Mg–Zn samples were solution

^{*} Corresponding author. Tel.: +61 7 3365 4197; fax: +61 7 3365 3888.

E-mail address: g.song@minmet.uq.edu.au (G. Song).

Table 1
Composition of magnesium alloys

Designation	Remarks	Mg	Al	Zn	Mn	Cu	Fe	Sn	Pb	Ni	Be	Cr	Zr	Sr
		wt. %	wt. %	wt. %	wt. %	wt. %	wt. %	wt. %	wt. %	wt. %	wt. %	wt. %	wt. %	wt. %
CP-Mg	Commercial purity magnesium ingot	Bal	0.007	<0.005	0.015	<0.002	0.020	<0.002	<0.002	<0.001	<0.001	<0.001	<0.002	<0.001
CP-Mg1Al	Commercial purity Mg1Al alloy	Bal	1.11	<0.005	0.016	<0.002	0.015	<0.002	<0.002	<0.001	<0.001	<0.001	<0.002	<0.001
Mg1Al-HT1	Commercial purity Mg1Al alloy after solution heat-treatment	Bal	5.08	<0.005	0.010	<0.002	0.020	<0.002	<0.002	<0.001	<0.001	<0.002	<0.002	<0.001
Mg5Al-HT1	Commercial purity Mg5Al alloy after solution heat-treatment	Bal	10.0	<0.005	0.010	<0.002	0.020	<0.002	<0.002	<0.001	<0.001	<0.002	<0.002	<0.001
Mg10Al-HT1	Commercial purity Mg10Al alloy after solution heat-treatment	Bal	0.010	0.48	0.017	<0.002	0.017	<0.002	<0.002	<0.001	<0.001	<0.001	<0.002	<0.001
Mg0.5Zn	Commercial purity Mg0.5Zn alloy	Bal	0.009	0.99	0.017	<0.002	0.015	<0.002	<0.002	<0.001	<0.001	<0.001	<0.002	<0.001
Mg0.5Zn-HT1	Commercial purity Mg0.5Zn alloy after heat-treatment	Bal	0.010	2.38	0.015	<0.002	0.020	<0.002	<0.002	<0.002	<0.001	<0.001	<0.002	<0.001
Mg1Zn	Commercial purity Mg1Zn alloy	Bal	0.010	2.38	0.015	<0.002	0.020	<0.002	<0.002	<0.002	<0.001	<0.001	<0.002	<0.001
Mg1Zn-HT1	Commercial purity Mg1Zn alloy after heat-treatment	Bal	<0.01	0.008	<0.01	<0.002	<0.01	<0.002	<0.002	<0.005	<0.001	<0.001	<0.002	<0.001
Mg2Zn	Commercial purity Mg2Zn alloy	Bal	1.14	<0.005	<0.005	<0.005	<0.005	<0.002	<0.002	<0.001	<0.001	<0.001	<0.002	<0.001
Mg2Zn-HT1	Commercial purity Mg2Zn alloy after heat-treatment	Bal	<0.01	0.008	<0.01	<0.002	<0.01	<0.002	<0.002	<0.005	<0.001	<0.001	<0.002	<0.001
HP-Mg	High purity magnesium ingot	Bal	<0.01	0.008	<0.01	<0.002	<0.01	<0.002	<0.002	<0.005	<0.001	<0.001	<0.002	<0.001
HP-Mg1Al	High purity Mg1Al alloy	Bal	1.14	<0.005	<0.005	<0.005	<0.005	<0.002	<0.002	<0.001	<0.001	<0.001	<0.002	<0.001

heat-treated at 425 °C for 24 h followed by quenching in cool water. Heat-treated samples were given a <HT1> designation, such as Mg1Al-HT1, Mg5Al-HT1, Mg10Al-HT1, Mg0.5Zn-HT1, Mg1Zn-HT1 and Mg2Zn-HT1.

2.2. Anodisation

All anodic coatings were produced in a basic anodisation electrolyte mainly containing 1.0% KOH and 1.6% K₂SiO₃ after specimens were cleaned in a hot (~85 °C) solution containing 9% silicate, 12% borate and 12% sodium hydroxide for a few minutes. During anodisation, the anodising current density was controlled at 20 mA/cm² for 10 min, then 10 mA/cm² for 10 min and finally 5 mA/cm² for 10 min. After anodisation, the specimens were cleaned with demineralised water and dried.

2.3. Evaluation of corrosion performance

The corrosion performance of the magnesium alloys as-cast and after anodisation was assessed by salt spray test (SST) (according to ASTM B117-97) and salt solution immersion test (SIT) in 5% NaCl solution. The corrosion damage of the anodised alloys was rated according to ASTM D 1654-92. The weight loss of the unanodised alloys after SST or SIT was also measured. The corrosion products of the unanodised alloys after corrosion were cleaned in a solution of 200 mg/L CrO₃+10 g/L AgNO₃.

2.4. Microstructure

Optical metallography was carried out to reveal the microstructure of the unanodised alloys. The microstructures of the anodic coatings were examined using a Phillips XL30 scanning electron microscope (SEM) and a JEOL 6460 LA SEM.

2.5. Chemical composition and thickness

The chemical compositions of the coatings were determined using a Kratos AXIS ULTRA X-ray photon spectroscopy (XPS)

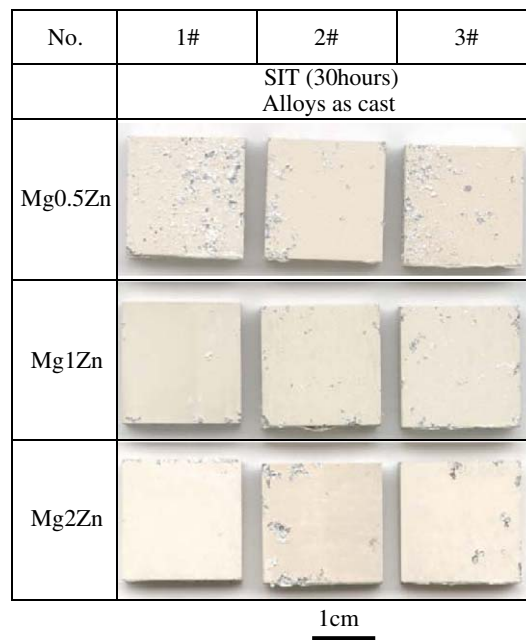


Fig. 2. Appearances of the anodised Mg–Zn alloys after immersion in 5% NaCl solution.

system. The XPS analysis was conducted after the coating surfaces were etched for 1 min by argon-ion-beam to reduce the carbon contamination.

The thickness of the anodic coatings was measured using a thickness gauge, PosiTector® 6000-FN1, which can measure the thickness of a film on non-ferrous substrates with an accuracy of ±0.1 μm.

3. Results

3.1. Corrosion resistance of the anodised alloys

3.1.1. Influence of iron impurity

Fig. 1 shows the corrosion morphologies of the anodised high purity and low purity alloys after exposure to 5% NaCl solution. The corrosion of the anodised alloys was localised, initiating from pitting especially at the edge or corner areas of

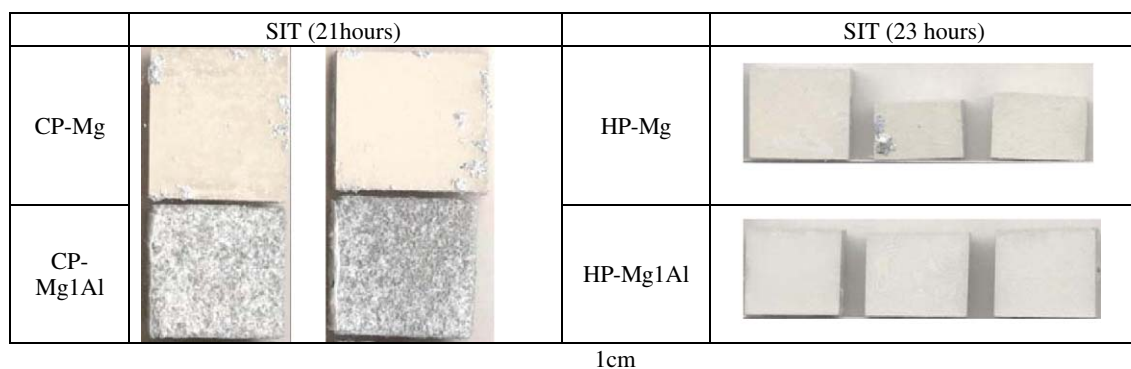


Fig. 1. Appearances of the anodised Mg–Al alloys after immersion in 5% NaCl solution.

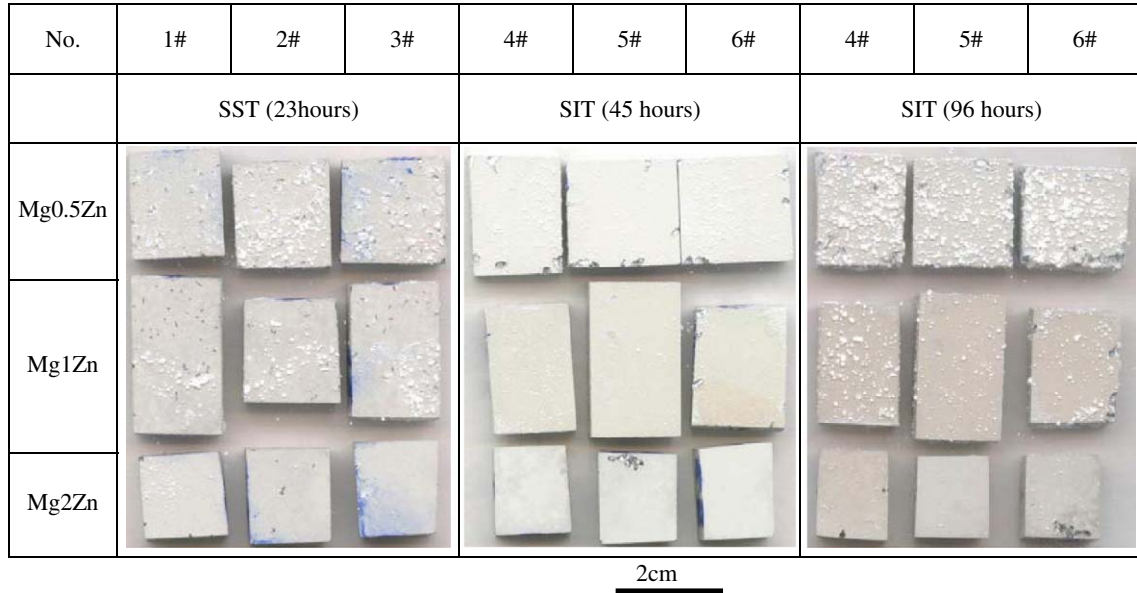


Fig. 3. Appearance of the heat-treated and anodised Mg–Zn alloys after exposure in SST and SIT.

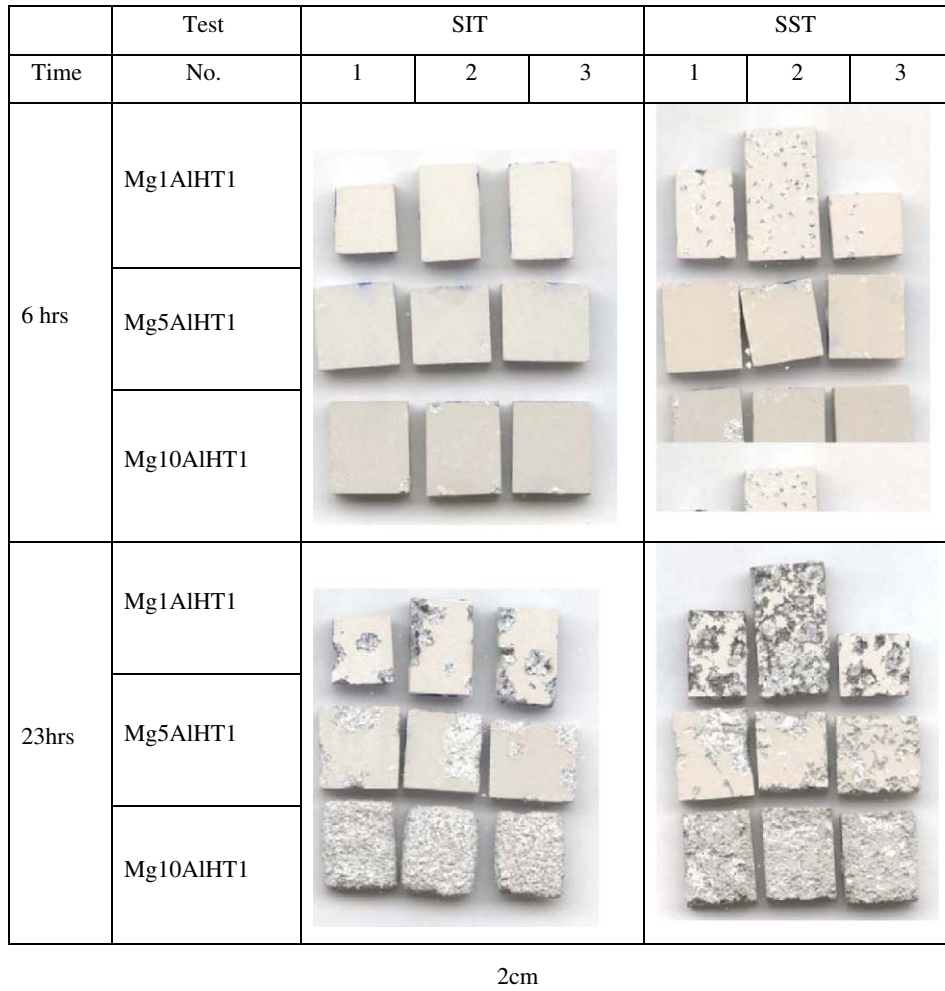


Fig. 4. Appearance of the anodised Mg–Al alloys after exposure in SST and SIT.

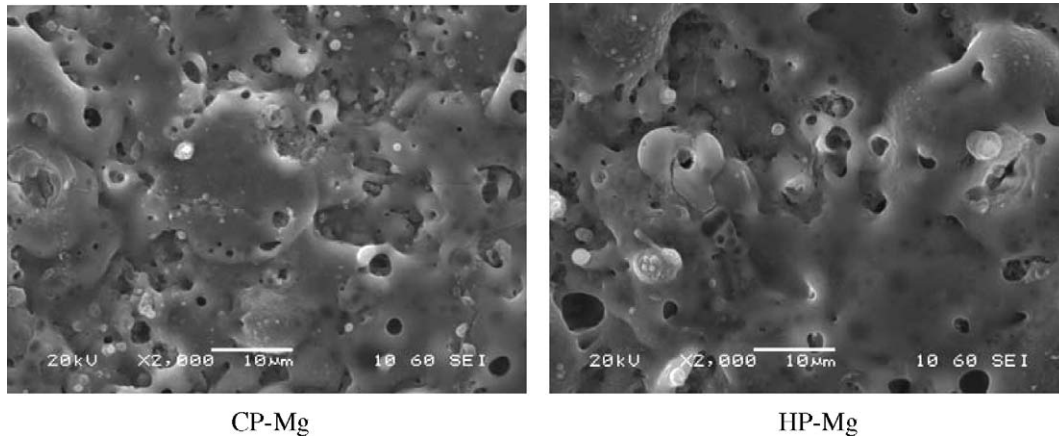


Fig. 5. The microstructure of the anodic coating on CP-Mg and HP-Mg.

the specimens. The corrosion subsequently developed into filiform corrosion and general corrosion. Both SST and SIT tests gave the same order of corrosion resistance; anodised HP-Mg and HP-Mg–Al were more corrosion resistant than anodised CP-Mg and CP-Mg–Al, indicating that the corrosion resistance of the anodised Mg alloys is determined by the iron impurity level of the alloy.

3.1.2. Aluminium effect

The appearance of the exposed specimens shown in Fig. 1 reveals that the corrosion resistance of the anodised CP-Mg1Al is lower than that of the anodised CP-Mg, whereas the anodised HP-Mg1Al is more corrosion resistant than the anodised HP-Mg.

3.1.3. Zn effect

Fig. 2 shows the corrosion morphologies of anodised Mg–Zn alloys, whose main feature was localised corrosion, initiating from pitting corrosion. Based on the SIT corrosion morphologies, the order of the corrosion resistance of the anodised alloys can be ranked as $Mg_2Zn \approx Mg_1Zn > Mg_{0.5}Zn$. The SST test also showed the same order of corrosion resistance of the anodised alloys.

3.1.4. Effect of solution heat-treatment

The corrosion morphologies of the heat-treated Mg–Zn alloys after anodisation are presented in Fig. 3. The corrosion behaviour of the anodised alloys was similar to that of the alloys without heat-treatment. The order of corrosion resistance of the anodised alloys appears to correlate with their zinc content: $Mg_2Zn-HT1 > Mg_1Zn-HT1 > Mg_{0.5}Zn-HT1$. Both the SST and SIT tests gave the same order of corrosion resistance. The results suggest that the corrosion resistance of the anodised alloys increased with increasing zinc content in the magnesium alloy. Comparison of the corrosion morphologies of the anodised as-cast Mg–Zn alloys with the heat-treated (HT1) alloys (see Figs. 2 and 3 (45 h)), indicates that the heat-treated anodised alloys are more corrosion resistant than the as-cast alloys. This could be associated with the homogenisation of the Zn distribution in the substrate alloys by the heat-treatment.

Fig. 4 presents the corrosion morphologies of the anodised Mg–Al alloys after solution heat-treatment. The corrosion resistance of the anodised Mg5Al-HT1 was higher than that of Mg1Al-HT1 and Mg10Al-HT1. The rating of the corrosion resistance is $Mg_5Al-HT1 > Mg_1Al-HT1 > Mg_{10}Al-HT1$. By comparing Figs. 4 and 1, it can be seen that the corrosion

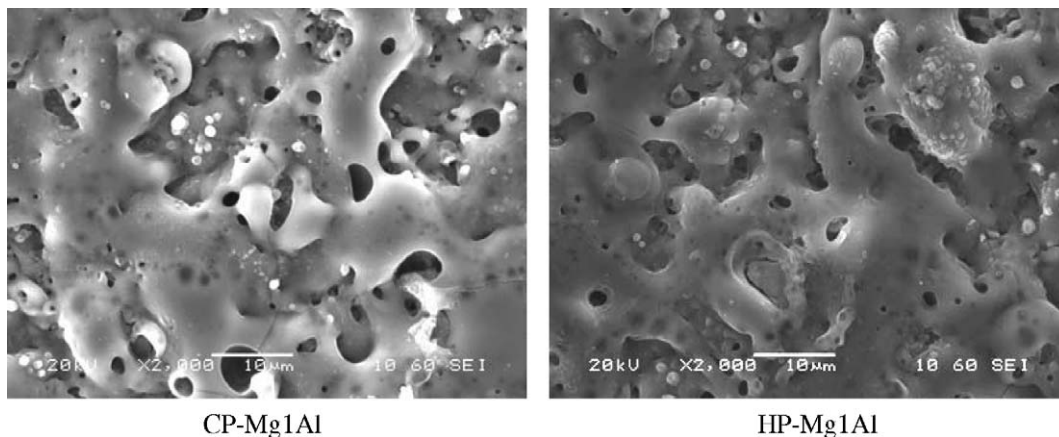


Fig. 6. The microstructure of the anodic coating on Mg–Al alloys.

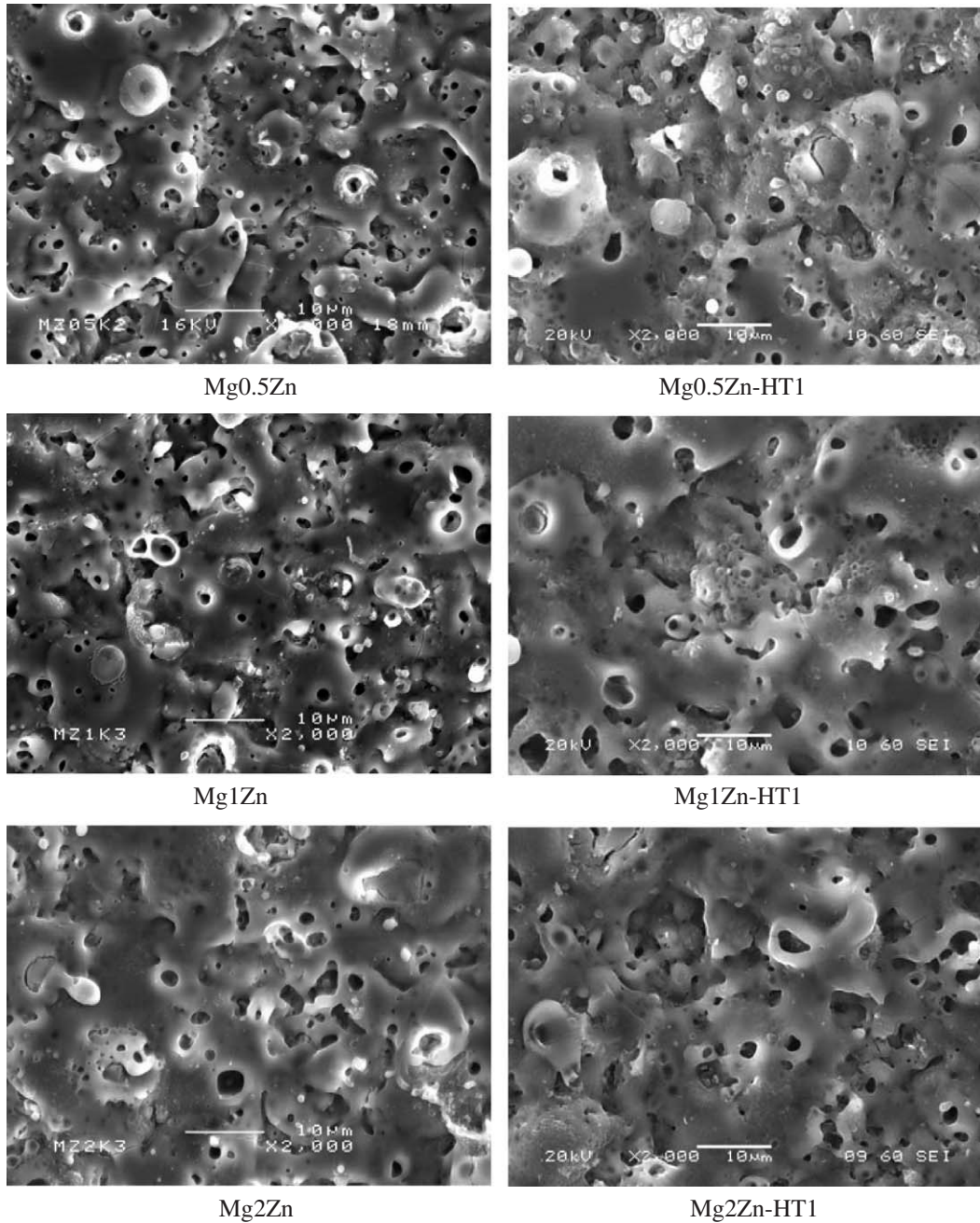


Fig. 7. The microstructure of the anodic coating on Mg–Zn alloys, as-cast and after solution heat-treatment.

resistance of the anodised Mg1Al un-heat-treated is lower than that of the anodised Mg1Al-HT1, which means that the solution heat-treatment also improved the corrosion resistance of the Mg–Al alloys. Figs. 4 and 1 also show that the anodised Mg5Al-HT1 has a corrosion resistance even lower than that of the anodised CP-Mg.

3.2. Microstructure of anodic coating

The microstructures of the anodic coatings on the Mg alloys as revealed by SEM examination (Figs. 5–8) are all similar. The anodic coatings are irregularly porous and some

pores are sealed. The diameters of the pores are in a range of several micrometers. The similar microstructures of all the anodic coatings on the different magnesium alloys suggest that the coatings should have a similar effect on the corrosion performance of all the alloys.

3.3. Chemical composition of anodic coating

In the study, the XPS detected area was about $3 \times 3 \text{ mm}^2$. In this area of an anodised coating, there were plenty of pores. The coating is thin inside the pores and thick outside the pores. Therefore, the measured XPS should be the average information

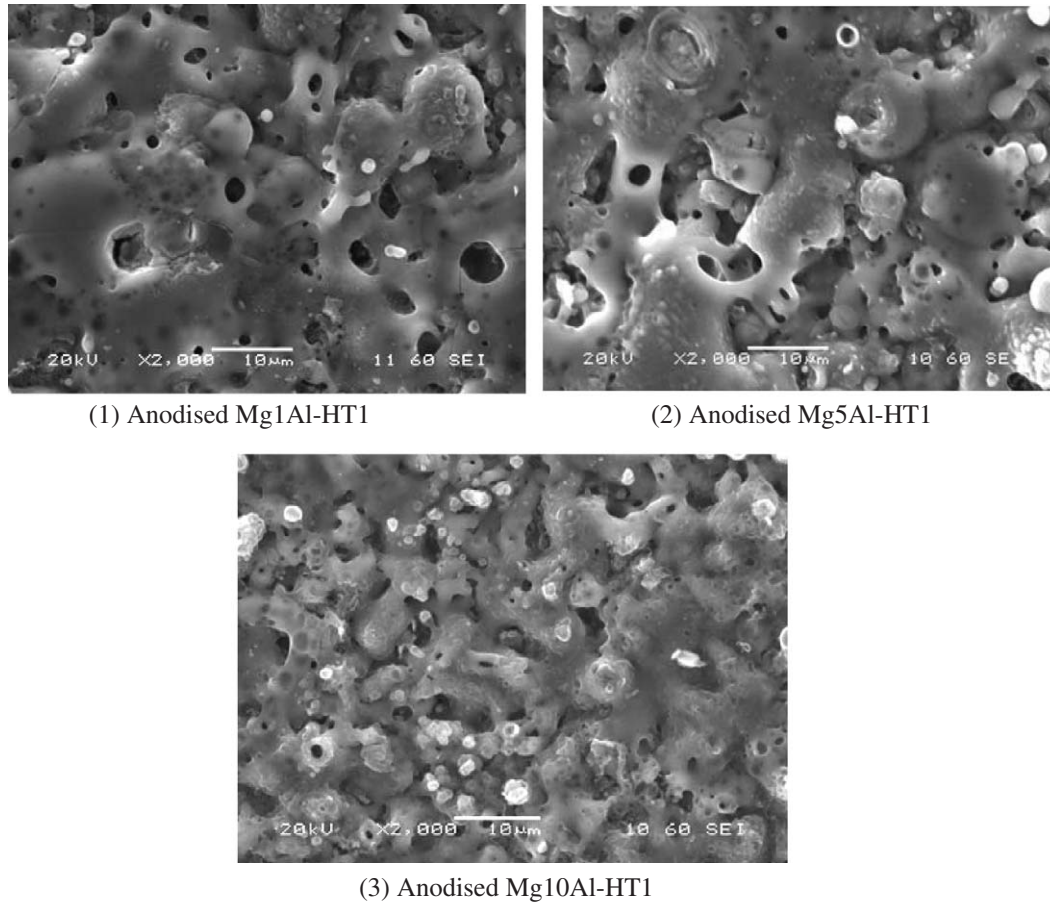


Fig. 8. The microstructure of the anodic coating on Mg–Al alloys after solution heat-treatment.

of the thick film outside the pores and the thin film inside the pores. Hence, the XPS results represent the average composition of an anodised coating.

The chemical compositions of the anodic coatings are listed in Table 2. The coatings are similar in chemical composition. A possible chemical formula of the coating could be Mg

Table 2
The chemical compositions of anodic coating on Mg alloys

	Atomic concentration (%)					Si/Mg <i>x</i>
	C	O	Si	Mg	K	
CP-Mg	18.03	59.06	16.33	4.03	2.55	4
CP-Mg1Al	28.62	51.13	13.65	6.59		2
HP-Mg	14.47	57.44	19.23	5.19	3.68	3.6
HP-Mg1Al	18.46	51.09	4.76	1.88	6.53 Na/7.53 B/9.85 ^a	2.2
Mg0.5Zn	4.37	62.46	23.33	6.90	2.93	3
Mg1Zn	2.84	62.81	25.21	5.86	3.28	4
Mg2Zn	4.3	59.27	36.25	6.97	3.23	5
Mg0.5Zn-HT1	5.04	67.79	21.42	5.75		3.7
Mg1Zn-HT1	6.53	66.88	21.18	5.41		3.9
Mg2Zn-HT1	4.1	67.00	16.60	12.31		1.35
Mg1Al-HT1	38.94	41.57	10.96	8.53		1.3
Mg5Al-HT1	31.04	47.32	15.78	5.86		2.7
Mg10Al-HT1	35.24	44.99	15.75	4.02		3.9

^a Boron and sodium found in the coating were from the pre-treatment solution.

(OH)₂·MgO·(SiO₂)_x. No aluminium was detected in the anodic coatings. The main difference was the content of silicon. The ratio of Si/Mg appeared to vary with the aluminium and zinc content. Our previous work [20] showed that the ratio of Si/Mg changed with the anodising process and that the silicate may be in the outer surface of a coating. The difference in the silicate content may cause a difference in corrosion resistance of the anodised alloy. However, in this study the relationship between silicate content in the anodic coating and the corrosion resistance of the coating is uncertain, which suggests that the composition of the coating may not be the main factor controlling the corrosion resistance of an anodic coating in this study.

3.4. Thickness of anodic coating

The thickness of all the anodic coatings was almost the same, about 20–22 µm. The similar thickness would be expected to have a similar effect on the corrosion performance. It cannot be the main factor causing a significant difference in the corrosion resistance of the anodised alloys.

3.5. Microstructure of substrate Mg alloys

Fig. 9 presents the microstructures of CP-Mg, HP-Mg and the Mg1Al alloys. They are single-phase alloys with a similar

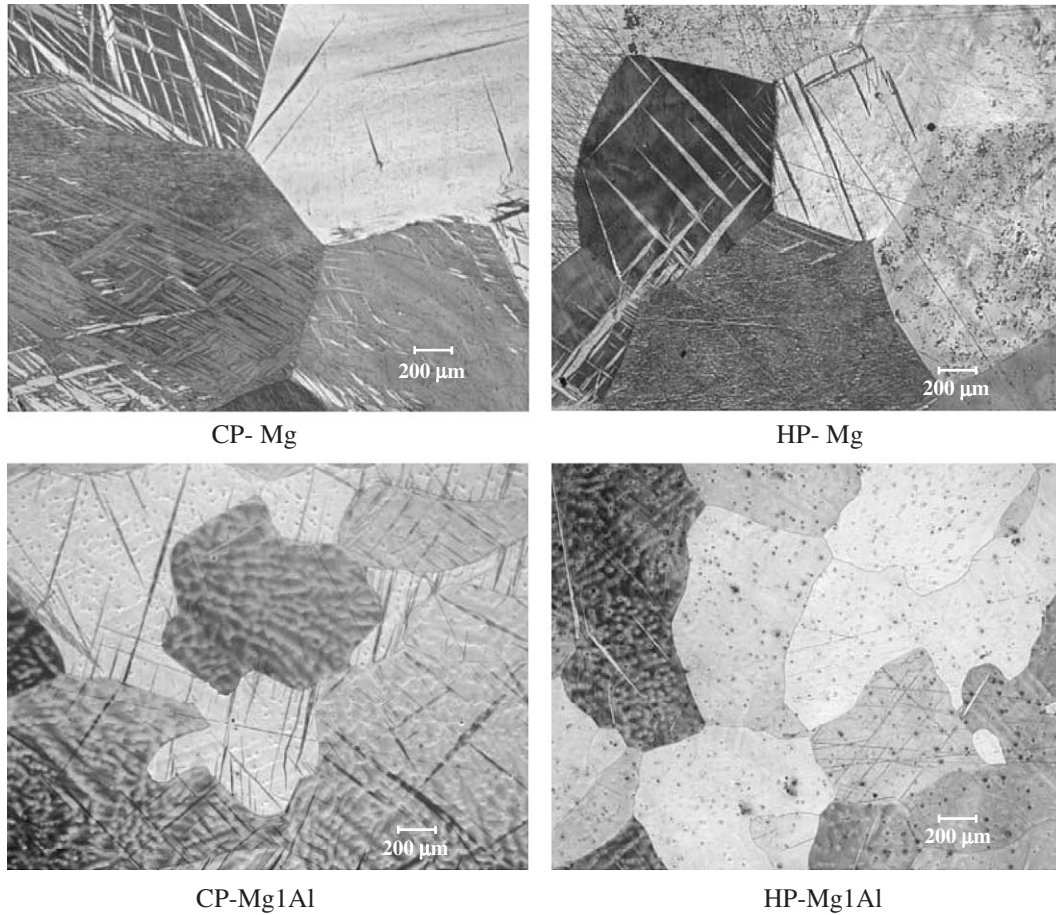


Fig. 9. Metallography of CP-Mg, HP-Mg and Mg1Al alloys.

grain size and shape. In particular, the microstructure of HP-Mg1Al alloy is similar to that of CP-Mg–Al alloys, which implies that the impurity iron did not affect the microstructure of the Mg1Al alloys.

Fig. 10 shows the microstructures of Mg–Zn alloys as-cast and after heat-treatment. The grain size decreases with increasing zinc content. These alloys are mainly single-phase, except for Mg2Zn that has some small second phase particles randomly distributed throughout the alloy. These particles were detected by EDS to be zinc rich eutectic precipitates. After heat-treatment, the grain shape and size did not change. However, the number of Zn eutectic particles in Mg2Zn was significantly reduced. The similarity in microstructure for Mg and Mg0.5Zn suggests that Zn in solid solution may be responsible for the different corrosion resistance of the anodised Mg and Mg0.5Zn.

Fig. 11 displays the microstructures of Mg–Al alloys as-cast and after heat-treatment. As-cast Mg1Al is a single-phase alloy, whereas Mg5Al contains some second phase particles, and Mg10Al has a significant amount of β phase along the grain boundaries. After heat-treatment, Mg1Al-HT1 remained a single-phase alloy, Mg5Al-HT1 became a single-phase alloy and Mg10Al-HT1 still had a smaller amount of β phase.

3.6. Corrosion resistance of substrate Mg alloys

The corrosion resistance of the Mg and Mg1Al alloys as indicated by weight loss under SIT and SST conditions is presented in Fig. 12(a). The corrosion rates of HP-Mg and HP-Mg1Al are lower than those of CP-Mg and CP-Mg1Al. Table 1 indicates that the Fe content was the main difference between CP and HP alloys. This suggests that the increased iron content was responsible for the increased corrosion rate, which is consistent with that reported in literature [12].

The corrosion rate of CP-Mg was higher than that of CP-Mg1Al in both SST and SIT testing conditions. For HP-Mg–Al alloys, the corrosion rate of HP-Mg was higher than that of HP-Mg1Al in SIT but lower than that of HP-Mg1Al in SST, but these differences were probably within experimental error.

Fig. 12(b) shows that increasing zinc content decreases the corrosion rate and the heat-treated alloys corroded at lower rates than those of the as-cast alloys. The improved corrosion resistance by heat-treatment can be attributed to a more homogeneous distribution of zinc in the heat-treated alloy.

After heat-treatment the corrosion rate of the Mg–Al single-phase alloys decreased slightly with increasing aluminium

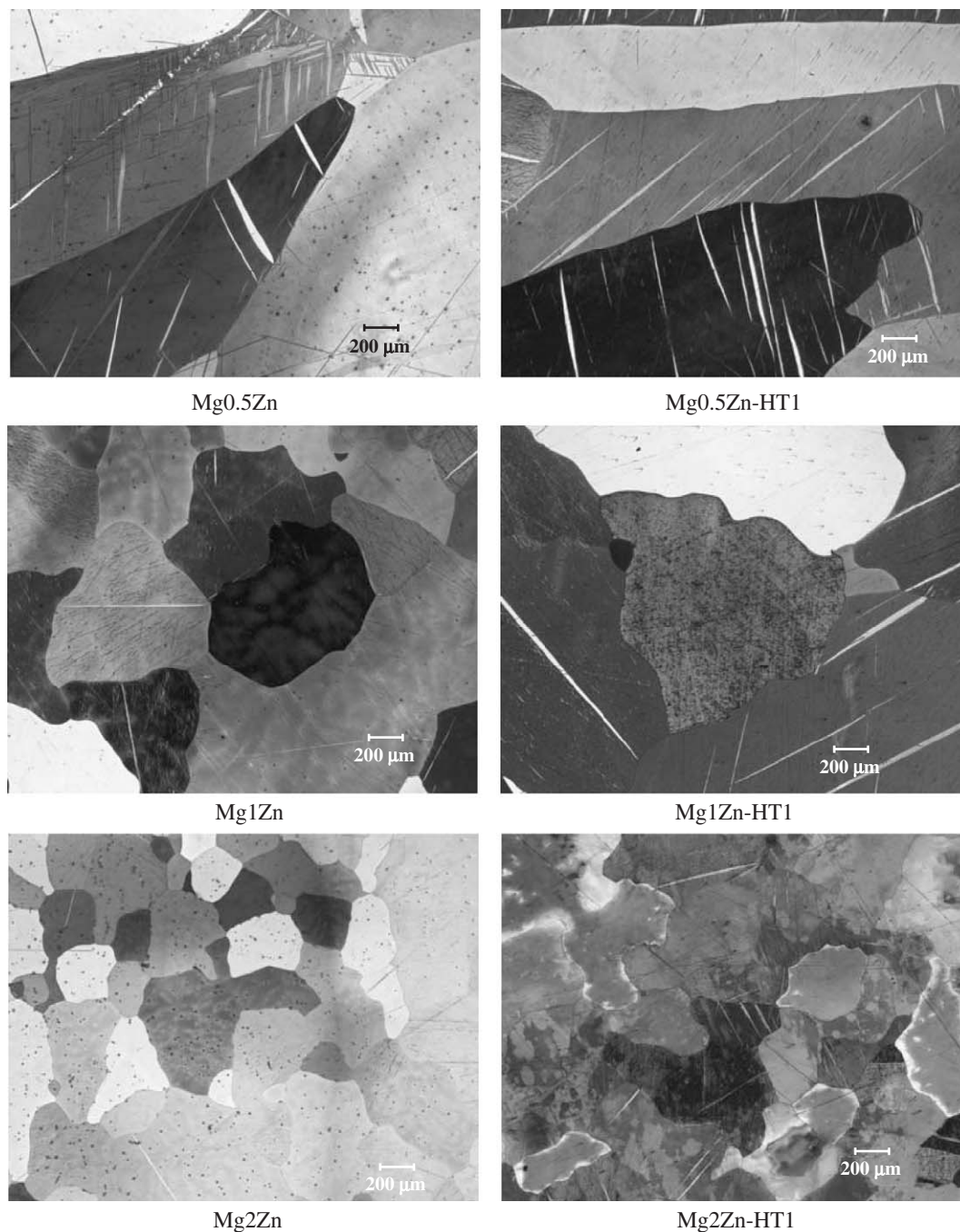


Fig. 10. Metallographic photos of Mg–Zn alloys as-cast and after heat-treatment.

content in the α matrix, hence the corrosion rate of Mg1Al was slightly higher than that of Mg5Al. If β phase is present, the corrosion rate increased again, so the corrosion rate of Mg10Al was slightly higher than that of Mg5Al.

4. Discussion

4.1. Effect of iron impurity on corrosion resistance

The results in Sections 3.1 and 3.6 indicate a similar dependence of corrosion resistance of Mg–Al alloys and that of the anodised Mg–Al alloys on the impurity level. The

microstructures of the substrate alloys and the anodic coatings, the chemical compositions and the thicknesses of the coatings on the HP-Mg–Al alloys were almost the same as those on the CP-Mg–Al alloys. Therefore, the different corrosion rates of the anodised HP and CP alloys could only be due to their different impurity contents. It seems that the anodic coatings played a blocking role for the corrosive media. Once the corrosive media had penetrated through the porous anodic coatings, the corrosion rates of the anodised alloys were determined by the corrosion resistance of the alloys. Thus, the impurity iron played an important role in determining the corrosion resistance of the anodised Mg–Al alloys.

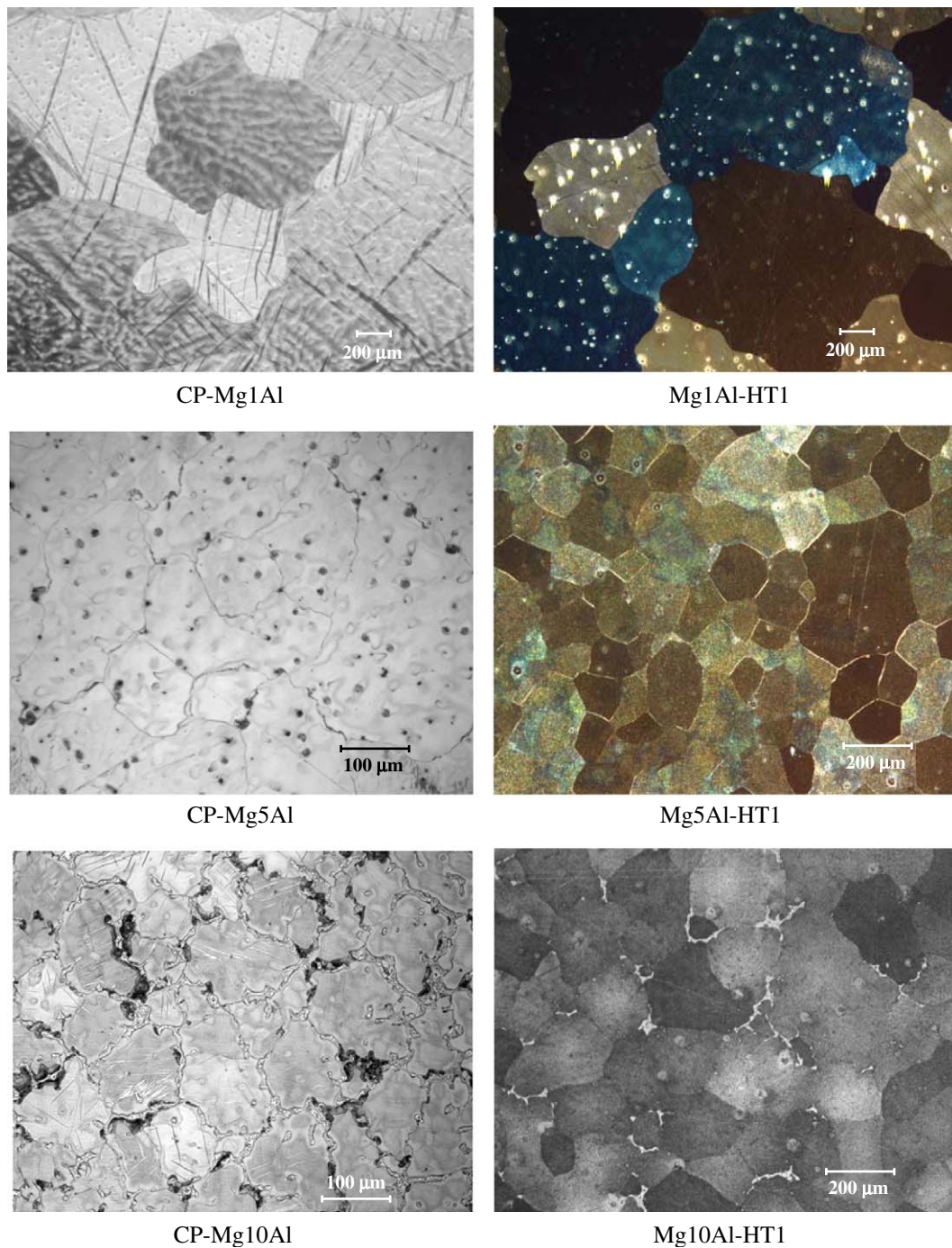


Fig. 11. Microstructures of Mg–Al alloys as-cast and after solution heat-treatment.

4.2. Effect of aluminium in single-phase alloys on corrosion resistance

The lower corrosion rate of CP-Mg1Al than that of CP-Mg (Fig. 12) can probably be associated with the lower impurity level of CP-Mg1Al (Table 1). This interpretation is substantiated by the result that HP-Mg1Al had a corrosion rate comparable to HP-Mg (Fig. 12). In HP-Mg, the impurity level was already low, so after it was alloyed with aluminium, the impurity level could not be further lowered.

After anodisation, the corrosion resistance of HP-MgAl was higher than HP-Mg, which is contradictory to the corrosion behaviour of the non-anodised alloys. This could be due to the slightly different coating compositions formed on HP-MgAl and HP-Mg (Table 2).

4.3. Effect of zinc on corrosion resistance

Zinc has a high over-potential for hydrogen evolution. The addition of zinc into the solid solution of the α matrix phase may increase the over-potential of hydrogen evolution of Mg

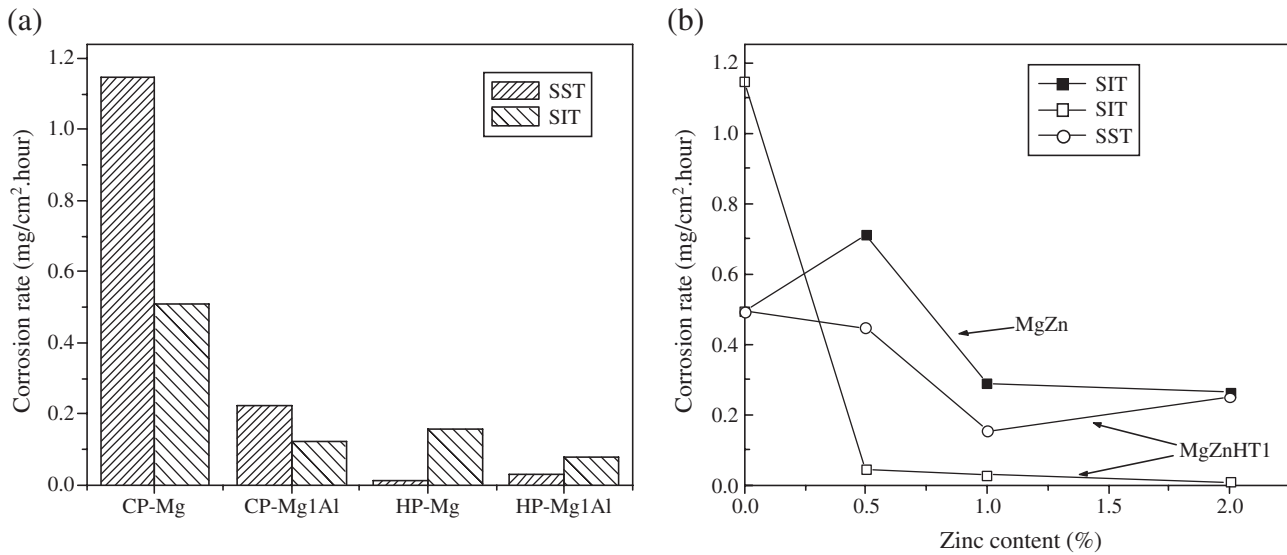


Fig. 12. Weight loss rates of the unanodised magnesium alloys under SIT and SST conditions after 6 h exposure.

alloys. Hence, the addition of Zn will not lead to an increased corrosion rate of the α phase of a magnesium alloy. On the other hand, a discrete precipitate normally results in microgalvanic corrosion and consequently causes an increase in corrosion rate of the alloy. However, since Zn has a high hydrogen over-voltage, the galvanic accelerating effect of Zn-rich particles is insignificant and therefore there is no evident increase in corrosion rate for an alloy containing Zn-rich particles. This may explain why the Zn containing alloy Mg2Zn, which contained some Zn-rich particles precipitated in the grains, did not exhibit an increased corrosion rate compared with Mg1Zn and Mg2Zn-HT1.

The corrosion resistance of the Mg–Zn alloys and that of the anodised alloys had a similar dependence on the zinc content. This further confirms that the corrosion resistance of the anodised alloys was dependent on the corrosion resistance of the substrate alloy.

In addition to the influence of the substrate, the corrosion resistance of the anodised alloy can normally be related to the microstructure, chemical composition and thickness of the coating. Since the microstructures and the thicknesses of the anodic coatings were almost the same, it was only the difference in the chemical composition of the coating that could affect the corrosion resistance. Table 2 shows that the content of silicate in the coating increases with increasing zinc content of the alloy. The higher level of silicate in the coating on Mg2Zn could lead to better protection for the anodised Mg2Zn alloy.

4.4. Effect of solution heat-treatment on corrosion resistance

For Mg–Zn alloys, heat-treatment resulted in a more uniform distribution of Zn and fewer Zn-rich particles in the alloy. Therefore, the corrosion resistance of the heat-treated Mg–Zn alloy after anodisation was improved (Fig. 12). This is also consistent with the conclusion that limited Zn alloying in the phase is beneficial to the corrosion performance of a Mg–Zn alloy [12].

For Mg–Al alloys, solution heat-treatment is expected to result in more uniform chemical composition and an increased content of aluminium in the matrix. The fact that the corrosion rate of Mg5Al-HT1 in SIT decreased slightly (see Fig. 13) could be attributed to the increased aluminium content in the matrix and/or the disappearance of β phase in the matrix [21]. The corrosion rate of Mg10Al-HT1 was slightly higher than that of Mg5Al-HT1 (Fig. 13) because there was still a significant amount of β phase in the alloy.

4.5. Relationship in the corrosion resistance of a magnesium alloy before and after anodisation

A comparison between the corrosion resistance of the anodised magnesium alloys (Figs. 1–4) and the corrosion rates of the unanodised magnesium alloys (Figs. 12 and 13) indicates that there is a close relationship between the corrosion resistance of an alloy before and after anodisation. To reveal the

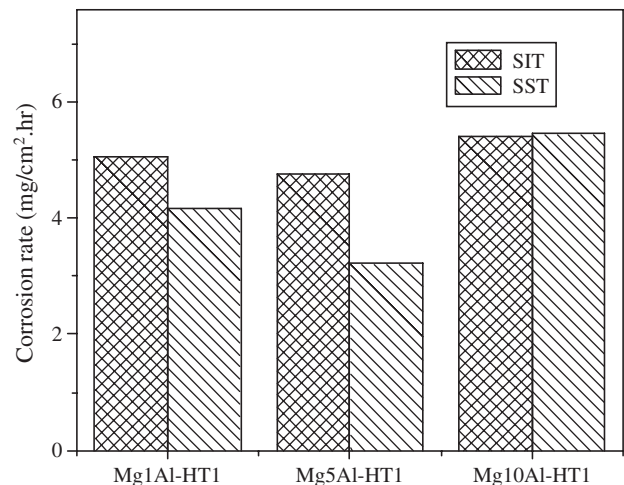


Fig. 13. The corrosion rates of unanodised solution heat-treated Mg–Al alloys after under SIT and SST conditions after 6 h exposure.

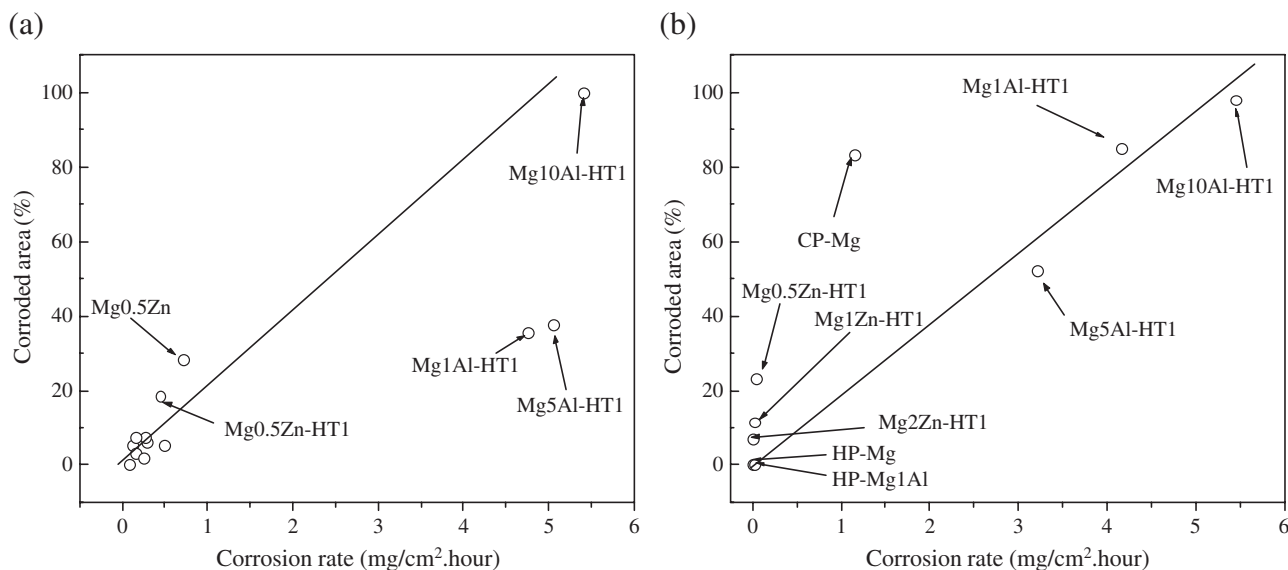


Fig. 14. Percentage of the corroded area of the anodised alloys vs. the corrosion rate of the unanodised substrate alloy under (a) SIT, (b) SST conditions.

dependence of the corrosion resistance of an alloy after anodisation on that of the alloy before anodisation, the corroded areas of coating are plotted against the weight loss rate of the substrate alloy. Fig. 14 shows that the percentage of the corroded area of the anodised alloys increases linearly with the corrosion rate of the substrate alloys. Only Mg1Al-HT1 and Mg5Al-HT1 alloys deviate from the line under the SIT condition. This could be attributed to the very deep corrosion pits formed on these two alloys. In SST, the corroded areas of the anodised alloys are also related linearly to the corrosion rates of the substrates. These results suggest that an anodic coating due to its porosity only acts as an incomplete blocking layer. The corrosive solution can get into the coating and reach the substrate through the pores [20]. Therefore, the corrosion resistance of the substrate plays a critical role in the corrosion performance of the anodised alloy. This explains why anodisation cannot change the dependence of corrosion resistance on the alloying elements aluminium and zinc (see Figs. 12 and 13).

5. Conclusions

1. The presence of impurity iron in Mg–Al alloys decreases the corrosion resistance of the alloys after anodisation.
2. Alloying aluminium in the commercial purity Mg–Al matrix phase decreased the corrosion resistance of this alloy after anodisation.
3. Alloying aluminium in high purity Mg–Al matrix phase improved the corrosion resistance of the matrix after anodisation.
4. The solution heat-treatment of Mg–Zn, Mg1Al and Mg5Al alloys improved the corrosion resistance of these alloys after anodisation.
5. The anodic coatings provide an incomplete barrier to corrosion. The corrosion resistance of the anodic coatings was correlated with the corrosion performance of the substrate.

Acknowledgment

The research work was supported by UQIPRS and CAST scholarships. The authors would like to acknowledge the support of the Cooperative Research Centre for Cast Metals Manufacturing (CAST). CAST was established and is supported by the Australian Government's Cooperative Research Centres Program.

References

- [1] M. Takaya, *Keikinzoku* 37 (1987) 581.
- [2] F. Stippich, E. Versa, G.K. Wolf, G. Berg, C. Friedrich, *Surf. Coat. Technol.* 103–104 (1998) 29.
- [3] E.L. Schmeling, B. Roschenbleck, M.H. Weidemann. In United States Patent: 4978432, 1990.
- [4] S. Nakanishi. In *Jpn. Kokai Tokkyo Koho* (Japanese Patent): 11279795, 1999.
- [5] G.L. Kotler, D.L. Hawke, E.N. Aqua, *Light Met. Age* 34 (1976) 20.
- [6] G.R. Kotler, D.L. Hawke, E.N. Aqua, SDEC-77: 9th SDEC International Die Casting Exposition and Congress, MECCA Convention Center, Milwaukee, Wisconsin, vol. 9, 1977, p. G-T77.
- [7] P. Kurze, D. Banejee, *Oberflaechen Polysurf.* 39 (1998) 7.
- [8] O. Khaselev, D. Weiss, J. Yahalom, *J. Electrochem. Soc.* 146 (1999) 1757.
- [9] T.F. Barton, J.A. Macculloch, P.N. Ross. In US patent: 6280598, 2001.
- [10] G. Song, *Adv. Eng. Mater.* 7 (2005) 563.
- [11] G. Song, *Mat. Sci. Forum* 488–489 (2005) 649.
- [12] Z. Shi, G. Song, D. StJohn, A method for evaluating the corrosion resistance of anodised magnesium alloys, *Corrosion and Prevention 2001*, ACA, Newcastle, 2001, paper #058.
- [13] T.F. Barton, C.B. John, *Plating Surf. Finish.* 82 (1995) 138.
- [14] T.F. Barton. In US Patent: 5792335, 1998.
- [15] O. Khaselev, J. Yahalom, *Corros. Sci.* 40 (1998) 1149.
- [16] T. Minota, K. Yamaguchi, T. Kato. In *Jpn. Kokai Tokkyo Koho* (Japanese Patent): 2001123294, 2001.
- [17] M. Avedesin, H. Baker (Eds.), *Magnesium and Magnesium Alloys*, ASM Specialty Handbook, ASM International, Materials Park, OH, 1999.
- [18] O. Khaselev, D. Weiss, J. Yahalom, *Corros. Sci.* 43 (2001) 1295.
- [19] A.J. Zozulin, D.E. Bartak, *Met. Finish.* 92 (1994) 39.
- [20] Z. Shi, G. Song, A. Atrens, *Corros. Sci.* 47 (2005) :2760.
- [21] G. Song, A. Bowles, D. StJohn, *Mater. Sci. Eng., A Struct. Mater.: Prop. Microstruct. Process.* 366 (2004) 74.